Journal of Ovarian Research

RESEARCH

Open Access

Neoadjuvant chemotherapy induces phenotypic mast cell changes in high grade serous ovarian cancer

Julia McAdams[1], Jasmine Ebott[1,2], Corinne Jansen[1,2], Chloe Kim[3], Daniela Maiz[4], Joyce Ou[5], Linda C. Hanley[5], Payton De La Cruz[4] and Nicole E. James[1,2*]

Abstract

Background High grade serous ovarian cancer (HGSOC) is the most lethal gynecologic malignancy in which patients have still yet to respond meaningfully to clinically available immunotherapies. Hence, novel immune targets are urgently needed. Our past work has identified that mast cells are significantly upregulated at the mRNA level in HGSOC patient tumors following neoadjuvant chemotherapy (NACT) exposure. Therefore, in this current investigation we sought to characterize intratumoral mast cell phenotypic changes as a result of NACT exposure and determine how these adaptations are associated with patient clinical outcomes.

Methods Hematologic immunohistochemistry was employed to determine mast cell levels in 36 matched pre- and post-NACT HGSOC patient tumors. Fluorescent Immunohistochemistry was utilized to identify Tryptase+(carboxypeptidase A3 (CPA3) + mast cells as well as histamine levels in 29 and 20, respectively, matched pre- and post-NACT HGSOC patient tumors. Finally, human immortalized mast cells, LUVA were stimulated with carboplatin and paclitaxel and genomic changes were analyzed by quantitative PCR.

Results Hematologic labeled intratumoral mast cells were significantly upregulated in the intraepithelial and stromal regions of the tumor, post-NACT. Lower levels of pre-NACT mast cells were significantly associated with an improved progression-free survival (PFS). Histamine, a marker of mast cell degranulation was similarly upregulated in post-NACT exposed tumors. Through the characterization of mast cell specific proteases Tryptase and CPA3, it was found that Tryptase+/ CPA3 + mast cells were significantly upregulated both in the intraepithelial and stromal compartments of the tumor, while Tryptase + cells were significantly upregulated in the stromal regions of the tumor. Lower post-NACT treated levels with Tryptase+/ CPA3 + cells were significantly associated with improved overall survival (OS) and PFS while higher Tryptase + mast cells were associated with improved OS. Finally, following chemotherapy exposure mast cell activating factors *AREG* and *CCL2* were significantly upregulated while *TGFB1*, an inhibitor of mast cell activation was downregulated in LUVA cells.

*Correspondence:
Nicole E. James
nejames@carene.org

Full list of author information is available at the end of the article

Conclusions Enhanced mast cell numbers, as well as activation and degranulation are a consequence of NACT exposure. Post-NACT mast cells displayed differing associations with survival outcomes that was dependent upon granule classification. Ultimately, mast cells represent a clinically relevant putative HGSOC immune target.

Keywords Mast cells, High grade serous ovarian cancer, Neoadjuvant chemotherapy

Introduction

High grade serous ovarian cancer (HGSOC) possesses the highest mortality rate of all gynecologic malignancies due to the fact that patients are frequently diagnosed at an advanced stage and develop chemo-resistant disease within 18 months following frontline therapy [1]. While the past decade has led to the incorporation of both angiogenic and poly-ADP-ribose polymerase (PARP) inhibitors as standard of care maintenance therapies, with the exception of patients that are defined homologous recombination deficient, HGSOC as a whole has only seen a slight improvement in progression-free survival (PFS). Moreover, while immunotherapies such as programmed cell death protein 1 (PD-1) have revolutionized clinical care in cancer subtypes such as melanoma and non-small cell lung cancer, PD-1 based inhibitors have only shown modest response rates at best in HGSOC [2]. Nevertheless, HGSOC is considered an immune responsive cancer as it has been extensively documented that intratumoral T cells are related to improved survival outcomes [3, 4]. Therefore, the muted response that HGSOC exhibits to clinically available immunotherapies has been attributed to the immunosuppressive nature of the ovarian tumor immune microenvironment (OTIME). However, despite the fact that the OTIME retains cytotoxic lymphocytes it is also composed of a high degree of T regulatory cells (Tregs), cancer associated fibroblasts (CAFs), and adipose tissue that all directly influence tumor immune evasion [2]. In an effort to better understand the unique nature of the OTIME and identify novel immune targets, our past analysis sought to evaluate genomic and immune cell changes in HGSOC patient tumors following neoadjuvant chemotherapy (NACT) exposure [5]. Interestingly, this study revealed that mast cells were significantly upregulated in post-NACT HGSOC patient tumors compared to matched pre-NACT treated diagnostic biopsy specimens [5].

Canonically, mast cells are involved in innate allergic responses like anaphylaxis and originally derived from CD34+bone marrow myeloid precursor cells that then migrate to peripheral tissues where they differentiate and mature under the instruction of tissue specific cytokines and chemokines [6]. As tissue-resident immune cells, mast cells have the unique ability to interact with the surrounding tissue microenvironment and can be located near blood vessels [6]. In addition, mast cells are characterized as having a diverse set of secretory granules such as histamines, cytokines, heparin, lysosomal enzymes, and notable proteases, tryptase and chymase. Unlike in anaphylaxis, where mast cells degranulate rapidly, within the context of cancer this process can occur in a gradual manner which in turn can have profound impacts on the local tumor immune microenvironment [7]. Interestingly, despite the potential mast cells possess to modulate the tumor immune microenvironment, this class of immune cells are dramatically understudied within the oncology field, as well as HGSOC specifically. Therefore, in this current investigation we sought to begin to characterize phenotypic mast cells changes in response to HGSOC NACT in order to begin to understand this immune cell subset's role in HGSOC.

Methods

Cell culture

Immortalized human mast cell line (LUVA) was purchased from Applied Biological Materials (ABM). Cells were maintained in StemPro-34 SFM (ThermoFisher Scientific, 10639011) supplemented with 2mM of L-glutamine, 10,000 U/ml of Penicillin-Streptomycin, and 50 mg of Primocin (InvivoGen, ant-pm-05). Cells were maintained in a 37 °C/5% CO2 humidified chamber. LUVA cells were treated with 100 µm of carboplatin (Santa Cruz Biotechnology, CAS 4157.5-94-4) and 10nM of paclitaxel (NIH Developmental Therapeutics Drug Cancer panel), with DMSO (Sigma Aldrich, D54879) used as a corresponding control. All treatments were for 48-hours. Cell viability analysis was performed to ensure that the chemotherapy treatment did not lead to a significant decrease in LUVA cell viability (Supplementary Fig. 1). Viability was assessed after the 48-hour timepoint with the addition of 10ul/well of CellTiter 96® Aqueous One Solution cell proliferation MTS assay (Promega, G3580O). Subsequently, cells incubated for 1 h at 37 °C/5%CO_2 and read at 492 nm to assess viability.

Patient samples

A total of 36 and 29 matched HGSOC pre-and post-NACT formalin-fixed, paraffin-embedded (FFPE) patient tumors were included in this retrospective study, for the hematologic mast cell stain, and Tryptase/Carboxypeptidase A3 (CPA3) staining, respectively. Histamine staining was performed in 20 patients from the original 36 patient cohort used for the hematologic mast cell stain. By definition of HGSOC, all patients included in this analysis had grade 3 disease. Pre-NACT specimens were from

Table 1 Patient clinical outcomes hemotoxic mast cell stain

	***N* (% of total 36 patients)**
Stage	
IIIA	1 (3%)
IIIB	5 (14%)
IIIC	25 (69%)
IV	5 (14%)
Recurred	
Yes	32 (89%)
No	4 (11%)
Overall Survival Status	
Living	11 (30%)
Deceased	23 (64%)
Lost to Follow up	1 (3%)
Deceased not from HGSOC	1 (3%)
	Median [Range]
Age at Diagnosis	63 [46–79]
PFS (months)	16 [6–51]
OS (months)	40 [12–83]

Table 2 Patient clinical outcomes tryptase and CPA3 immunostaining

	***N* (% of total 29 patients)**
Stage	
IIIA	1 (3%)
IIIB	2 (7%)
IIIC	20 (69%)
IV	6 (21%)
Recurred	
Yes	27 (93%)
No	2 (7%)
Overall Survival Status	
Living	6 (20%)
Deceased	23 (80%)
	Median [Range]
Age at Diagnosis	63 [46–79]
PFS (months)	15.5 [8–51]
OS (months)	37 [12–83]

the patient's diagnostic biopsy and post-NACT treatment tumors were obtained at the patient's interval debulking surgery. Pre-NACT tumors were obtained via diagnostic laparoscopy or exploratory laparotomy, as appropriate for the clinical scenario and individual surgeon discretion. All patients received frontline carboplatin and paclitaxel therapy. All tissue was obtained, and respective experiments managed under The Women and Infants Hospital Review Board protocol approval #1817644-11. Detailed patient clinical outcomes for the hematologic-based mast cell stain and Tryptase/CPA3 stain, are shown in Tables 1 and 2, respectively.

Immunohistochemistry

A commercially available combined eosinophil-mast cell hematologic staining kit (ab150665) was used to evaluate mast cell levels in 36 matched pre- and post-NACT FFPE HGSOC tumors. Staining was performed following the manufacturer's protocol, without the optional step of counterstaining in Hematoxylin (Modified Mayer's solution). In this kit mast cells were defined as bright blue, eosinophils were defined as bright red, and nuclei stained a dull blue.

Fluorescent immunohistochemistry

Fluorescent Immunohistochemistry to evaluate histamine levels and Tryptase+/CPA3+cells in 29 matched pre- and post-NACT FFPE HGSOC tumors was performed as previously described in [5, 8]. Primary and secondary antibodies along with respective dilutions were as follows:

Tryptase (Abcam, ab2378, 1:50).

CPA3 (Abcam, ab251685, 1:50).

Histamine (Novus Biologicals, NBP2-45266, 1:50).

Anti-Rabbit DyLight™488 (Vector Laboratories, DI-1488, 1:1,000).

Anti-Mouse DyLight™594 (Vector Laboratories, DI-2594, 1:1,000).

Microscopy

The mast cell hematologic staining was visualized and imaged using an Evos M5000 Fluorescence imaging system using a 20x objective. Histamine and corresponding DAPI images were acquired with a spinning disk confocal Nikon Eclipse Ti microscope at a 10x objective. Finally, Tryptase, CPA3, and corresponding DAPI images were obtained from a Zeiss Axio Imager M1 and were acquired using diode lasers 402, 488, and 561 using a 20x objective. Representative images for Tryptase+/CPA3+mast cells were taken at a 40x objective.

Image analysis

Ten randomly selected fields were captured for each slide for the hematologic based stain. Mast cells that were bright blue were counted and Women and Infants Hospital staff pathologists were consulted if any mast cells were in question. For histamine intensity and Tryptase+/CPA3+mast cell counts, three and ten randomly selected fields per case were selected based on DAPI staining, respectively. All images were processed using Image J. For histamine intensity, image analysis was performed on grayscale 8-bit images and were thresholded for specific staining, with mean and integrated optical density (IOD) calculated. For Tryptase+/CPA3+mast cells, the total number of positive tryptase, CPA3, and Tryptase+/CPA3+cells were counted per field. Examples of images of matched HGSOC patient pre- and post-NACT tissue used to quantify Tryptase+/CPA3+cells can be seen in Supplementary Figs. 2–4.

Quantitative PCR

RNA isolation and subsequent quantitative PCR was performed as previously described [5]. Validated human primers were purchased from Bio-Rad (*AREG*, *CCL2*, *TGFβ1*, *VEGFA*, *TNF*, *IL-2*, *CCL7*, *IL-10*, *TGFβ2*). Custom primer sequences (Invitrogen) are as follows:

18s rRNA-F-CCGCGGTTCTATTTTGTTGG.
18s rRNA-R-GGCGCTCCCTCTTAATCATG.

Statistical analysis

GraphPad Prism was employed for all statistical analyses. Student-t-tests were performed to determine differences in pre- and post-chemotherapy exposed HGSOC patient tissue and LUVA cells. Kaplan-Meier survival curve analysis was performed to assess hematologic mast cell counts and Tryptase and Tryptase/CPA3 positive mast cells with PFS and OS with log-rank p-values, hazard ratios and 95% confidence intervals determined. All p-values reported were 2-tailed and unadjusted.

Results

Intraepithelial and stromal mast cells are increased following NACT exposure

We performed a commercially available hematologic-based immunohistochemical assay in matched pre- and post- NACT treated tumors in order to validate our findings from our previous study [5] that demonstrated an increase in mast cells post-NACT at the mRNA level. Representative images of mast cells both pre- and post-NACT HGSOC patient tissue can be seen in Fig. 1A. Corroborating our previous study, we previously found a significant ($p=0.0098$) increase in average positive mast cells per field post-NACT (Fig. 1B) In addition, it was also found that both intraepithelial and stromal mast cells were significantly ($p<0.05$) increased post-NACT exposure (Fig. 1C). Overall, this immunohistochemical analysis allowed for us to determine that mast cells are located post-NACT exposure both in the stromal and intraepithelial compartments of the tumor, which differs greatly from T- cells subsets which are well known to be predominantly located in the stromal regions of the tumor [9]. Interestingly, this analysis showed that unlike T cell subsets, mast cells appear to make it into the intraepithelial compartments of the tumor, which implies that they have the potential to directly impact surrounding tumor cells. Upon the examination of mast cell levels and their association with patient clinical outcomes we observed no significant relationships with progression-free survival (PFS) or overall survival (OS) upon stratification by upper and lower quartile post-NACT mast cells counts (Supplementary Figs. 5–6). In addition, we identified that patients with lower levels of pre-NACT total (HR=2.544[1.013–6.388], log-rank p-value=0.006) and intraepithelial (HR=3.278[1.226–8.765], log-rank p-value=0.018) mast cells experienced a significantly longer PFS (Fig. 2A-B). However no significant associations between total or intraepithelial pre-NACT mast cells and OS were detected (Fig. 2C-D). The association between stromal pre-NACT mast cells and survival outcomes

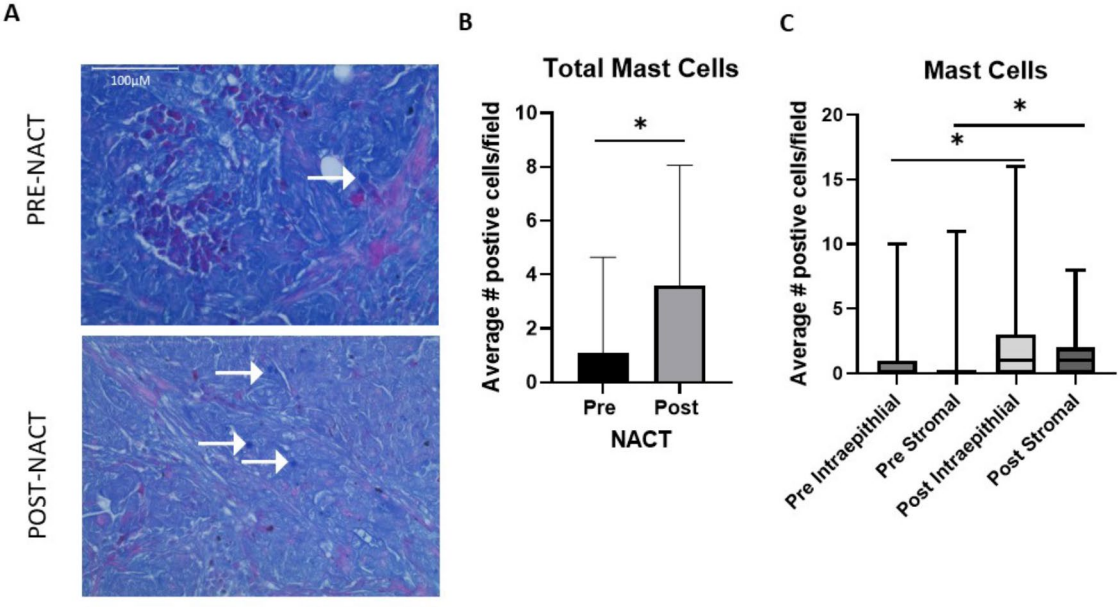

Fig. 1 Intratumoral stromal and intraepithelial mast cells are upregulated following chemotherapy exposure. (**A**) Representative images of hematologic mast cell staining in 36 matched pre- and post-NACT HGSOC patient tumors. Mast cells were depicted by a bright blue stain, while eosinophils were stained bright red and nuclei of cells a dull blue. Average number of positive (**B**) total and (**C**) intraepithelial and stromal mast cells pre- and post-NACT. Statistically significant differences determined by Student T-test. NACT, neoadjuvant chemotherapy, *$p<0.05$, as indicated

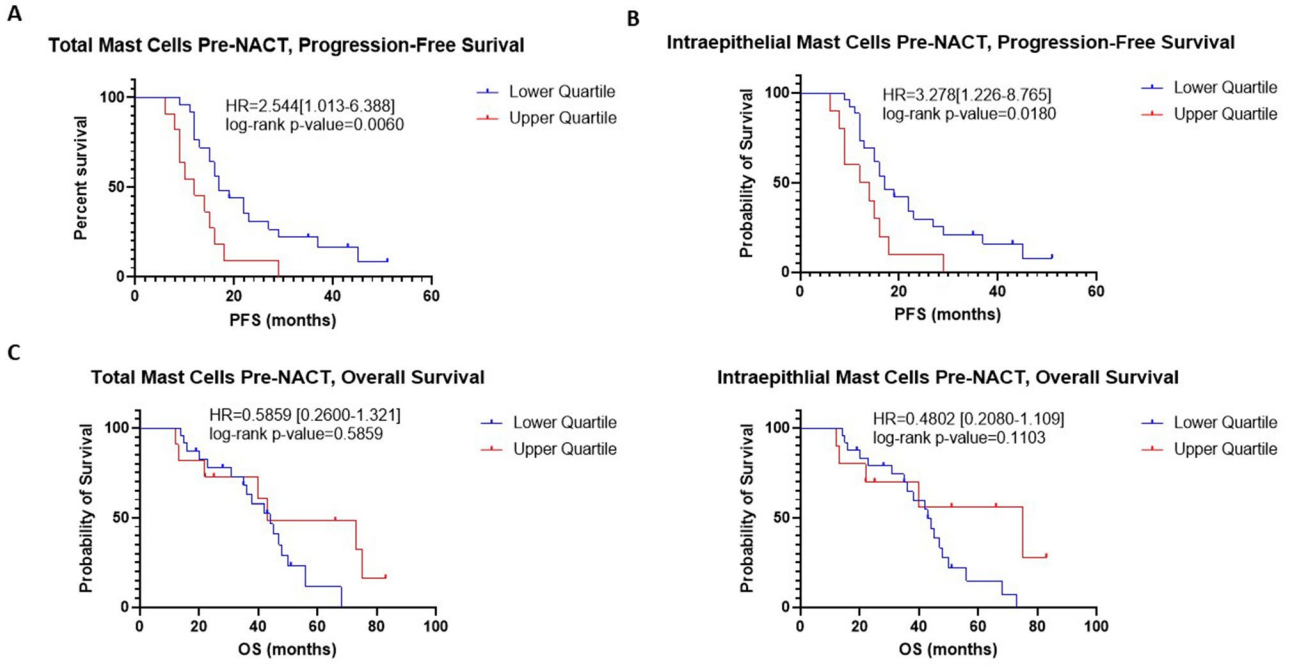

Fig. 2 Patient survival outcomes associated with pre-treatment hematologic mast cell levels. Kaplan-Meier curve analysis of pre-treatment (**A**) total (**B**) intraepithelial mast cells association with progression free survival stratified by lower and upper quartile. Kaplan-Meier curve analysis of pre-treatment (**C**) total and (**D**) intraepithelial mast cells association with overall survival stratified by lower and upper quartile. HR and associated log-rank p-values were reported. HR, hazard ratio

could not be determined as too few positive mast cells were observed (Supplementary File 1).

Intratumoral histamine levels are increased post-NACT exposure

Next, we sought to uncover how mast cell degranulation was affected. In order to investigate this phenomenon, we examined intratumoral levels of a common mast cell granule, histamine, in matched pre- and post- NACT treated tumors (Fig. 3A). Despite exhibiting a relatively dim intratumoral stain, it was found that histamine expression was significantly upregulated following NACT both when examined by mean intensity ($p=0.0478$) and IOD ($p=0.0032$) (Fig. 3B-C). Overall, these findings suggest that in addition to a significant increase in mast cells following chemotherapy exposure, mast cell degranulation is similarly enhanced.

Fluorescent immunohistochemistry analysis of tryptase and CPA3 mast cells

Next, due to the fact that our previous hematologic-based mast cell stain did not allow for the assessment of granule composition, matched HGSOC pre- and post- NACT were stained using mast cell specific protease markers Tryptase and CPA3, in order to specifically evaluate if mast cells based on granule content were similarly upregulated following NACT exposure. Interestingly, it was found that there was a strikingly significant ($p=0.0003$) upregulation of Tryptase+/CPA3+mast cells post-NACT (Fig. 4A-B). Furthermore, we evaluated changes in Tryptase+/CPA3+mast cells based on intratumoral localization and found that Tryptase+/CPA3+mast cells were significantly ($p<0.05$) increased following NACT exposure both in the intraepithelial (Fig. 5A) and stromal (Fig. 5B) regions of the tumor. The vast majority of CPA3+cells were also Tryptase+, with a minute amount of single CPA3+cells (Supplementary File 1). Hence, changes in CPA3+mast cells pre- and post- NACT were not evaluated. Upon examining changes in total and stromal Tryptase+, both were found to be significantly ($p<0.05$) upregulated post-NACT exposure (Fig. 5C-D), while intraepithelial Tryptase+cells were not ($p=0.0576$), but similarly exhibited higher levels post-NACT (Fig. 5E). Overall, these results validated our previous hematologic stain that intratumoral mast cells are indeed increased following chemotherapy exposure in both the stromal and intraepithelial compartments.

Furthermore, Kaplan-Meier survival curve analysis was performed, which revealed that total levels of Tryptase+/CPA3+mast cells post-NACT stratified by median levels showed lower levels associated with improved OS (HR=2.23[0.8994–5.547], log-rank p-value=0.043, Fig. 6A). However no significant association was detected upon stratification by intraepithelial and stromal Tryptase+CPA3+mast cells (Fig. 6B-C) and upon stratification of upper and lower quartile (Supplementary Fig. 7). To

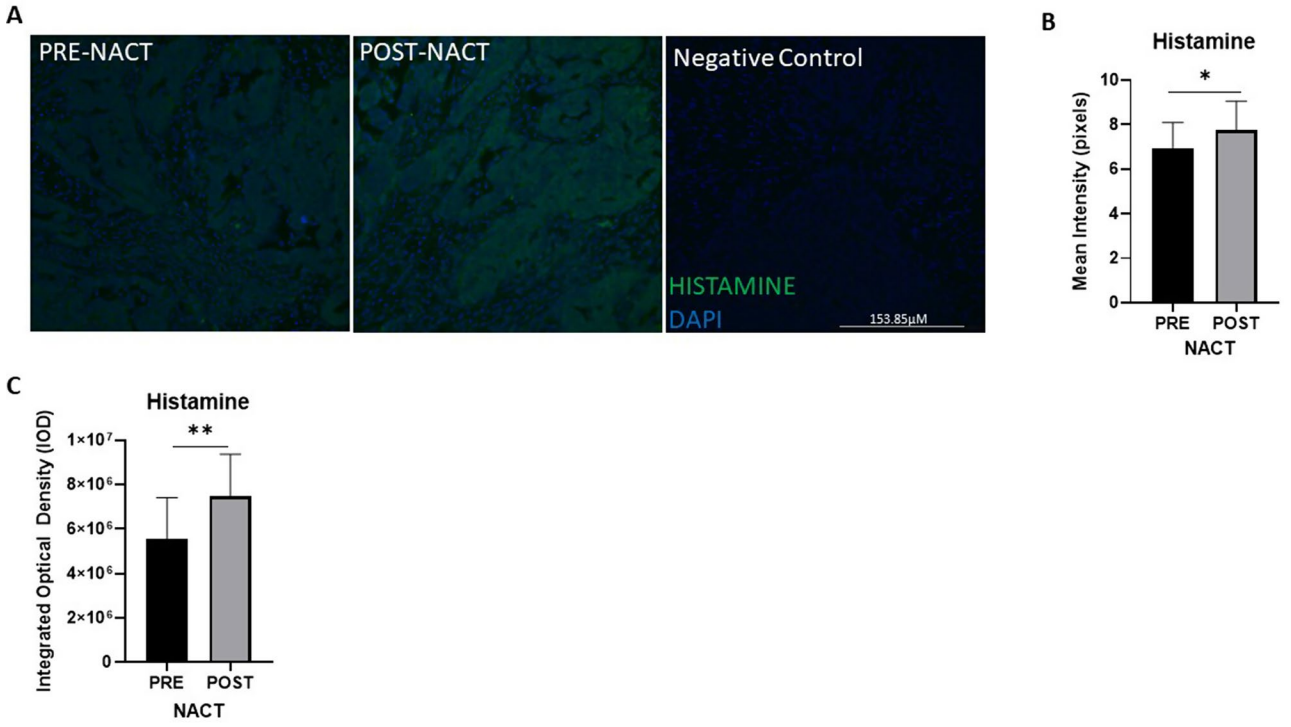

Fig. 3 Intratumoral histamine is upregulated following chemotherapy exposure (**A**) Representative immunofluorescence images of histamine expression in 20 matched pre- and post-NACT tumors and corresponding secondary only, negative control taken at a 10x objective. (**B**) Mean intensity (pixels) and (**C**) Integrated optical density of histamine in pre- versus post-NACT HGSOC tumors. Statistically significant differences determined by Student T-test. NACT, neoadjuvant chemotherapy, HGSOC, high grade serous ovarian cancer, $*p < 0.05$, as indicated

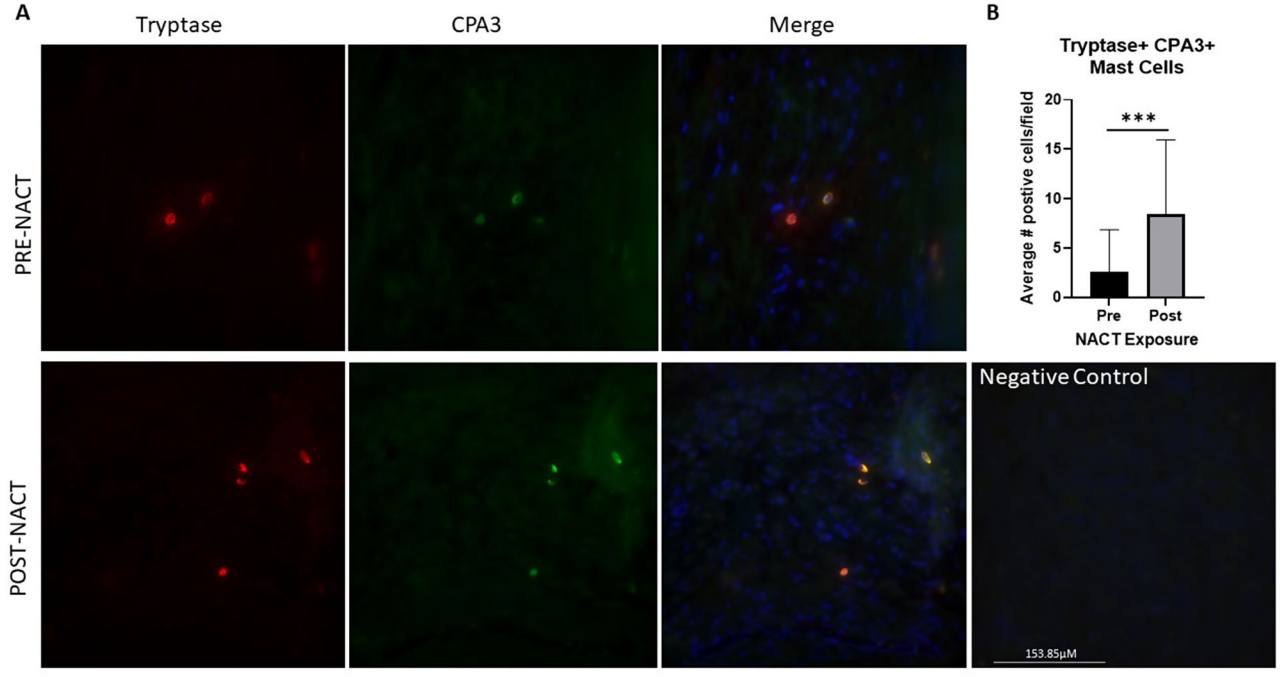

Fig. 4 Tryptase+/CPA3+mast cells are upregulated following chemotherapy exposure (**A**) Representative immunofluorescence images of Tryptase, CPA3 expression in 29 matched pre- and post-NACT tumors and corresponding secondary only, negative control taken at a 40x objective. (**B**) Average number of Tryptase+/CPA3+cells per field in matched pre-and post-NACT exposed HGSOC tumors. Statistically significant differences determined by Student T-test. NACT, neoadjuvant chemotherapy, HGSOC, high grade serous ovarian cancer, $***p < 0.0005$, as indicated

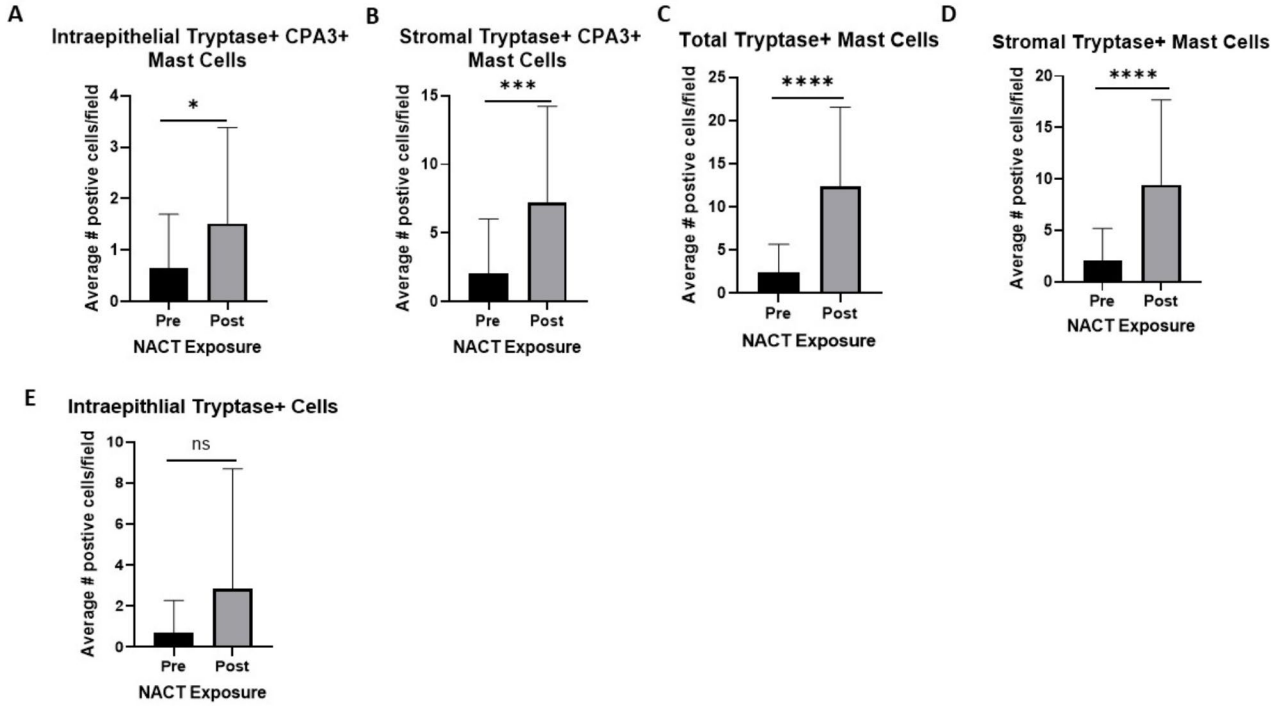

Fig. 5 Tryptase+/CPA3 + and Tryptase + cell subset expression in pre-and post-NACT HGSOC tumors. (**A**) intraepithelial and (**B**) stromal Tryptase+/CPA3 + mast cells in 29 matched pre- and post- NACT treated tumors. (**C**) total, (**D**) stomal, and (**E**) intraepithelial Tryptase + mast cells in 29 matched pre- and post- NACT treated tumors. Statistically significant differences determined by Student T-test. NACT, neoadjuvant chemotherapy, HGSOC, high grade serous ovarian cancer, * $p < 0.05$, *** $p < 0.0005$, **** $p < 0.00005$, as indicated, ns, non-significant

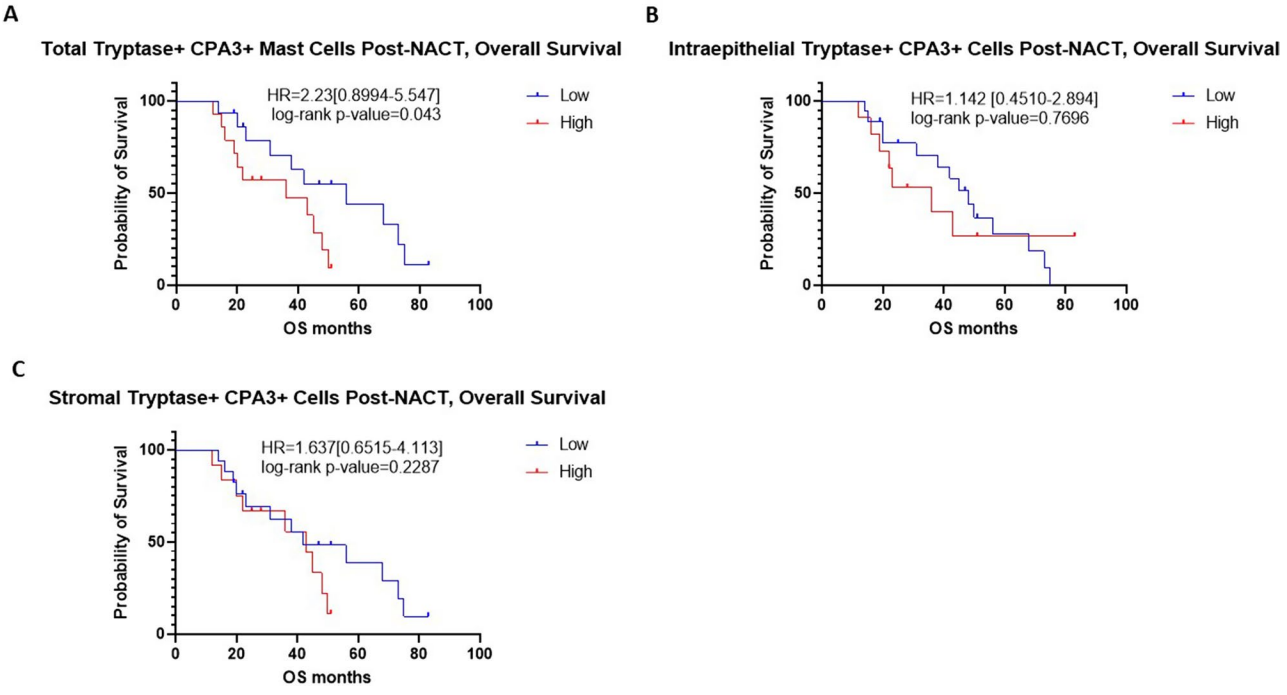

Fig. 6 Tryptase+/CPA3 + mast cells association with overall survival. Kaplan-Meier survival curve analysis of post-NACT (**A**) total, (**B**) intraepithelial, and (**C**) stromal Tryptase/CPA3 + mast cells association with overall survival stratified by median levels. HR and associated log-rank p-values were reported. NACT, neoadjuvant chemotherapy; HR, hazard ratio

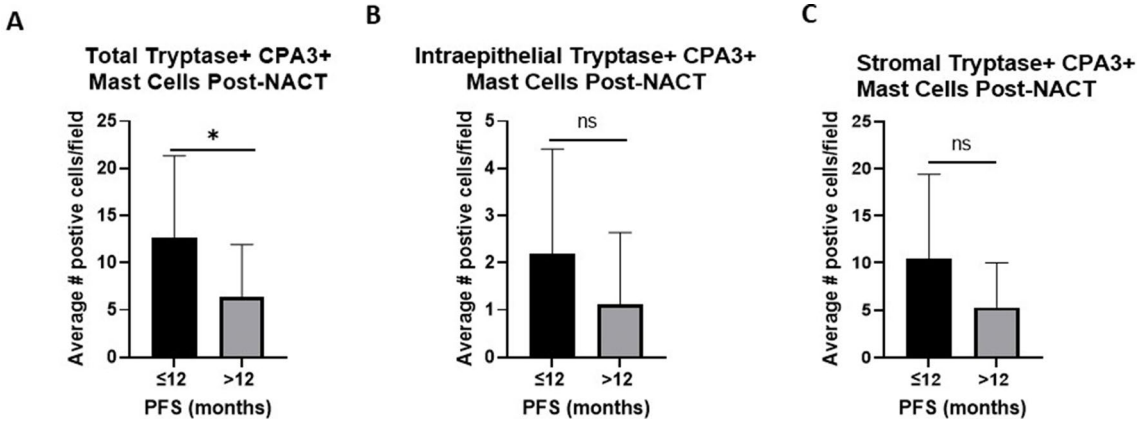

Fig. 7 Tryptase+/CPA3 + mast cells association with progression-free survival. Post-NACT (**A**) total, (**B**) intraepithelial, and (**C**) stromal Tryptase+/CPA3 + levels stratified by progression-free survival 12-month cut-off. Statistically significant differences determined by Student T-test. NACT, neoadjuvant chemotherapy, *$p < 0.05$, as indicated, ns, non-significant

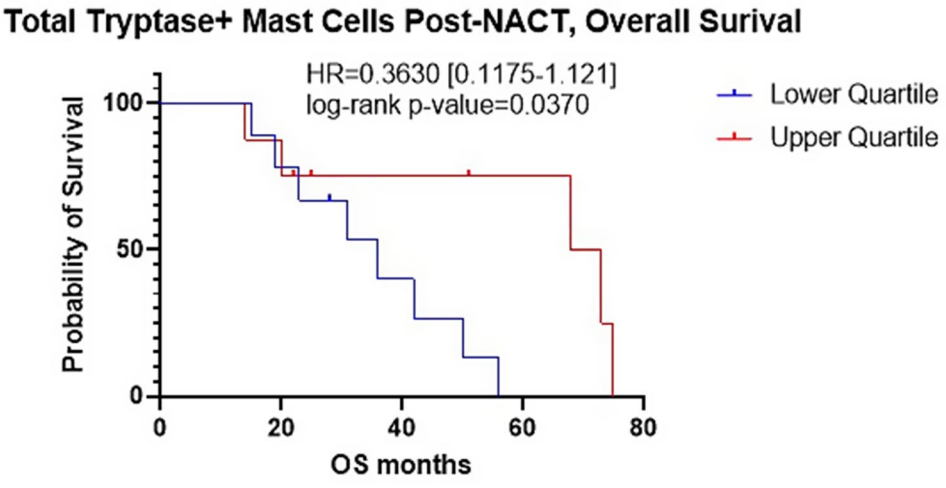

Fig. 8 Kaplan-Meier survival curve analysis of total post-NACT Tryptase + mast cells association with overall survival stratified by upper and lower quartile expression. HR and associated log-rank p-values were reported. NACT, neoadjuvant chemotherapy; HR, hazard ratio

assess mast cell counts with PFS we stratified patients by a lower-than-average HGSOC patient PFS of 12 months or less or an average PFS of over 12 months. Similar to what was observed from our Kaplan-Meier survival curve analysis, it was found that patients with a PFS of 12 month or under had a significantly higher mean total Tryptase+CPA3+mast cells compared to those with a PFS of over 12 months (12.64 positive cells per field versus 6.39 positive cells per field, $p=0.025$, Fig. 7A). While the same trend was observed with higher mean levels of both intraepithelial and stromal Tryptase+CPA3+mast cells in the 12 month or under PFS cohort, no statistically significant differences were detected (Fig. 7B-C). Interestingly, upon analysis of Tryptase+cells it was found that higher levels of total Tryptase+mast cells post-NACT were significantly associated with OS (HR=0.3630[0.1175–1.121], log-rank p-value=0.0370) upon stratification of upper and lower quartile level (Fig. 8). However, a significant association of total Tryptase+mast cells post-NACT and OS, was not detected upon stratification by median levels, or with PFS (Supplementary Figs. 8–10). Taken together, these results suggest that double positive Tryptase+/CPA3+mast cells hold differing prognostic significance in HGSOC than Tryptase+mast cells, highlighting the clinical implications of classifying mast cells by one versus two proteases.

HGSOC standard of care chemotherapy promotes mast cell activation

Finally, to complement our immunohistochemistry analysis we employed the human mast cell line, LUVA to determine how common mast cell derived factors change following treatment with standard of care HGSOC chemotherapies, carboplatin and paclitaxel. Interestingly, we saw a significant ($p=0.0017$) over 7-fold increase of amphiregulin (*AREG*), a low affinity EGFR ligand and

known mast cell activation factor [10] after exposure to chemotherapy (Fig. 9A). Similarly, a 7.5-fold significant ($p=0.015$) increase was observed in CCL2, which is known to be produced by mast cells upon IgE stimulation [11], was upregulated upon chemotherapy treatment (Fig. 9B) and *TGFB1*, a known inhibitor of mast cell activation [12] was significantly decreased (0.48-fold, $p=0.022$) post-chemotherapy treatment (Fig. 9C). Interestingly, despite the known effect that mast cells promote angiogenesis, we saw a significant decrease in *VEGFA* levels (0.66-fold, $p=0.0071$) (Fig. 9D). Furthermore, we observed a 1.76-fold increase in *TNF* which is associated with mast cell degranulation [13] following chemotherapy treatment, however this increase did not reach statistical significance (Fig. 9E). Finally, we observed no significant differences in other mast cell derived factors *IL-2*, *CCL7*, *IL-10*, and *TGFB2* (Fig. 9F-1).

Discussion

To the best of our knowledge, this current study is the first to not only establish that intratumoral mast cells are significantly upregulated in HGSOC following NACT, but that these mast cells exhibit unique phenotypic changes that are associated with activation, differentiation, and degranulation. There has been one functional study by Meyer et al. that utilized an in vivo murine ovarian cancer model to compare ID8 tumor cell growth in C57/BL6 WT and C57/BL6/ 6-Kit W-sh/W-sh mast cell deficient mice, and observed that the mast cell deficient mice exhibited a significant increase in ovarian tumor growth compared to their wild-type counterpart [14]. While the study does suggest that mast cells play a role in suppressing ovarian tumor growth, given the fact that these mice were devoid of all mast cells, this investigation cannot account for how specific mast cell phenotypes impact ovarian pathogenesis. Corroborating this finding that mast cells are beneficial for combating ovarian tumor growth, a translational study by the group Chan et al. found that higher levels of mast cell infiltration in advanced ovarian cancer patients that simultaneously had tumors with high levels of mean vessel density exhibited improved survival outcomes [15]. In contrast to this investigation, Cao et al. determined that stromal infiltrating mast cells were associated with poorer survival outcomes in HGSOC and significantly correlated with higher levels of intratumoral Tregs, M2 macrophages, and neutrophils, indicating a more immunosuppressive tumor immune microenvironment [16]. Interestingly, in both these studies, tryptase was employed to solely identify mast cells and yet led to differential associations with ovarian cancer patient survival. Supporting the discordance of these previous findings, this current study found that mast cells stained by a hemotoxic based assay and not granules, saw no significant association with survival

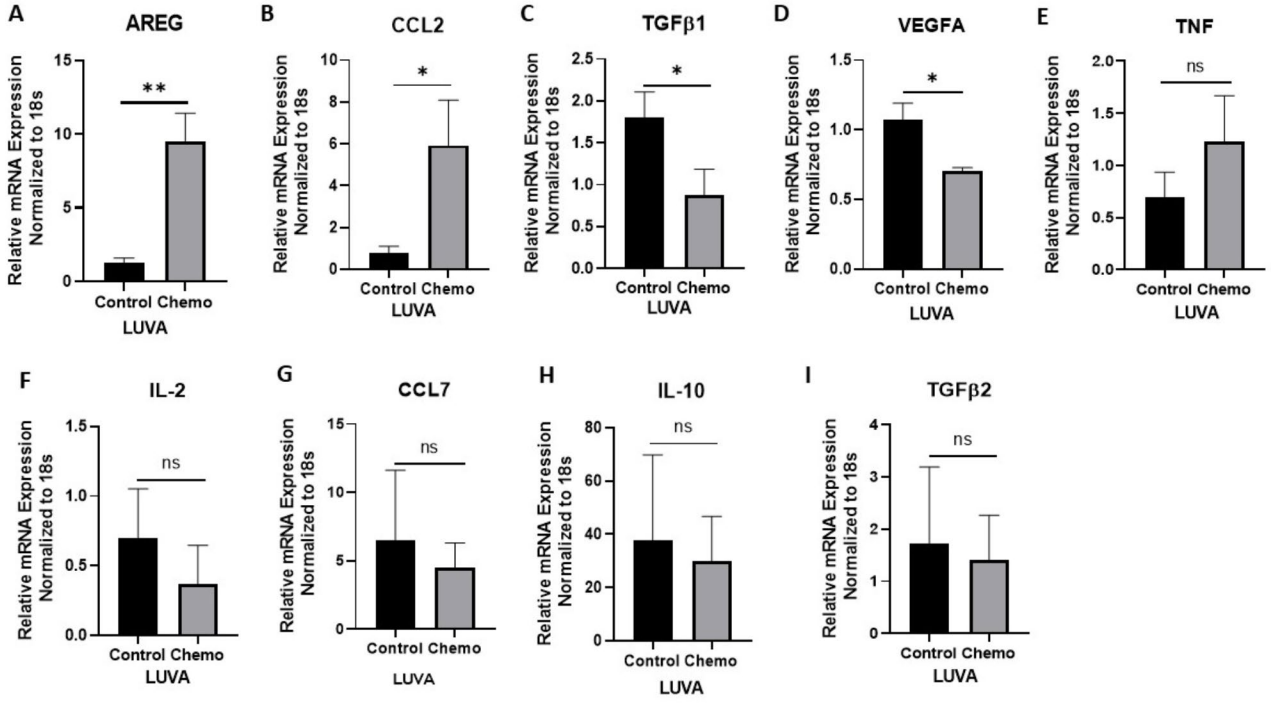

Fig. 9 qPCR analysis of LUVA mast cells exposed to standard of care HGSOC chemotherapy. (**A**) *AREG*, (**B**) *CCL2*, (**C**)*TGFβ1*, (**D**) *VEGFA*, (**E**) *TNF*, (**F**) *IL-2*, (**G**) *CCL7*, (**H**) *IL-10*, and (**I**) *TGFβ2* mRNA levels in LUVA cells stimulated with 100 µm of carboplatin and 10 nm of paclitaxel for 48h and analyzed via qPCR. Error bars represent standard deviation of ≥ 3 biological replicates. Statistically significant differences determined by Student T-test. NACT, neoadjuvant chemotherapy, HGSOC, high grade serous ovarian cancer, *$p < 0.05$, ** $p < 0.005$, as indicated, ns, non-significant

outcomes when examining post-NACT levels, but that higher pre-NACT levels of mast cells were associated with shortened PFS. Conversely, our study also found that post-NACT levels of Tryptase+CPA3+mast cells were associated with worse PFS and OS, while higher levels of Tryptase+cells exhibited an improved OS survival benefit. Overall, the discrepancy in these findings highlight the complexity of defining mast cells, as there are clear differing prognostic implications depending upon which granules are used to classify this cell subset. However, our findings clearly establish that a consequence of NACT exposure leads to the upregulation of intratumoral mast cells in HGSOC, underscoring that they could potentially be leveraged as a novel immune target.

Interestingly, previous research has shown that mast cell secretory granules are associated with cancer progression. Liu et al. found that histamine, a major mast cell secretory granule induces ovarian tumor cell proliferation through the upregulation of α and β estrogen receptors [17]. In addition, in an in vivo skin cancer model it was demonstrated that mast cell specific proteases chymase and tryptase levels increased at all stages of tumor development, in contrast to the number of mast cells which remained constant [18]. Furthermore, it was shown that tryptase has the ability to drive angiogenesis, as it was found to induce proliferation and migration of human umbilical cord vein endothelial cells (HUVECs) which was achieved through modulation of the JAK-STAT pathway [19]. Conversely, there is far less known about CPA3 in cancer pathogenesis. Unlike the serine proteases tryptase and chymase, CPA3 is characterized as a zinc-containing metalloproteinase that exhibits exopeptidase activity [20]. Moreover, it has been proposed that CPA3 could plausibly be utilized as a marker of mast cell differentiation as CPA3 levels are markedly increased upon maturation [21–24]. To the best of our knowledge, this current study was the first to examine intratumoral Tryptase+CPA3+mast cells in HGSOC, however, a recent study published by Atiakshin et al. reported the involvement of Tryptase+CPA3+mast cells in the formation of ovarian endometrioid cysts [25]. Moreover, one in vivo study discovered that the combination of mast cell chymase, tryptase and CPA3 was necessary in order to halt melanoma dissemination into the lung [26]. Overall, more investigations are crucial in order to elucidate the function and prognostic significance of this specific mast cell subset in cancer, and HGSOC specifically.

Despite the dual role that mast cells possess in terms of promoting and combating tumorigenesis, it has been proposed in recent years that mast cells play a key role in immunotherapy resistance as they contribute to an immunosuppressive tumor immune microenvironment [27]. A bioinformatic analysis by Li et al. found that mast cell levels correlated with PD-1 immunotherapy resistance in melanoma [28]. Furthermore, the group utilized an in vivo mouse model that discovered that treatment with cromolyn sodium, a mast cell stabilizer, increased PD-1 treatment efficacy [28]. A study by Somasundaram et al. corroborated these findings, postulating that mast cells could contribute to PD-1 therapeutic resistance in a melanoma model, which was explained by lower levels of HLA class I and co-localization of mast cells and Tregs [29]. As HGSOC patients have yet to respond meaningfully to clinically available immunotherapies, it is plausible that the high degree of intratumoral mast cells that we have identified in patient tumors post-NACT could potentially be one immunosuppressive factor that is compromising immunotherapeutic efficacy, as both in the frontline and recurrent setting an immunotherapy regimen would be given after standard of care chemotherapy.

In addition to immunotherapy, a study in pancreatic cancer demonstrated that mast cells reduce anti-angiogenic efficacy [30]. Specifically, it was found that mast cells secretion of granzyme B leads to the downstream release of angiogenic factors fibroblast growth factor 1 (FGF-1) and granulocyte-macrophage colony stimulating factor (GM-CSF) from the extracellular matrix [30]. Moreover, it was found that treatment with an anti-VEGF therapy reduced tumor volume more substantially when mast cells were deemed granzyme B deficient. However, when mice were treated with cromolyn sodium, a synergistic effect with the VEGF inhibitor was observed (30). This finding is of particular clinical relevance to HGSOC as bevacizumab is FDA approved to be used in both first and second treatment lines [31]. Despite this FDA approval, bevacizumab effect on PFS dissipates after 2 years and contributes to no improvement of OS ovarian cancer rates [32]. Alike to clinically investigated immunotherapies, bevacizumab is frequently given in the maintenance setting with or following chemotherapy. Hence, the high degree of mast cell activation, degranulation, and differentiation that we observe intratumorally, may contribute to an increase in angiogenesis that if targeted could potentially improve bevacizumab response rates in HGSOC.

One of the major limitations of this study was the small sample size of matched pre- and post-NACT HGSOC patient tissue used for the hemotoxic based mast cell stain and Tryptase/CPA3 stain. Therefore, an expanded cohort is necessary to determine how mast cells classified by differing granule contents post-NACT are associated with HGSOC patient survival outcomes. Furthermore, it will be imperative to determine how mast cells correlate with other immune cells subsets in HGSOC patient tissue both pre- and post-NACT. In addition, while our preclinical data revealed that human immortalized mast cells treated with chemotherapy leads to genomic

changes associated with mast cell activation, future studies in vivo are necessary in order to determine how the increase in mast cells and phenotypic changes impacts HGSOC chemotherapy response, as well as determining how factors associated with mast cell activation syndrome, prostaglandins and leukotrienes are impacted post-NACT. Finally, as mast cells are known to be present within the peritoneum specifically in regions known as "milky spots" that classified as permeable regions that permit contact of lymphatic tissue and peritoneal fluid [33], it will be important to examine mast cell levels in the ascites of HGSOC patients and associated phenotypic changes both pre-and post-NACT exposure.

Conclusion

This study strongly suggests that intratumoral mast cells are increased as a consequence of chemotherapy exposure, along with enhanced levels of activation, differentiation, and degranulation. Furthermore, this investigation highlights the importance of defining how intratumoral mast cells are characterized, as we observed differing associations with survival depending upon specific mast cell granule content. Overall, this study underscores the importance of this understudied immune cell subset in HGSOC and lays the foundation for future research to elucidate if targeting mast cells can improve HGSOC immunotherapy response and patient clinical outcomes.

Supplementary Information

The online version contains supplementary material available at https://doi.org/10.1186/s13048-024-01516-y.

Supplementary Material 1: Supplementary Figure 1. Cell Viability analysis of LUVA cells. LUVA cells stimulated with 100uM of carboplatin and 10nm of paclitaxel, with respective DMSO control for 48 hours

Supplementary Material 2: Supplementary Figure 2. Representative immunofluorescence images of Tryptase, CPA3 staining. Expression of Tryptase and CPA3 in 29 matched pre- and post-NACT tumors and corresponding secondary only, negative control taken at a 20x that were used for quantification of tryptase and CPA3 positive cells

Supplementary Material 3: Supplementary Figure 3. Representative immunofluorescence images of Tryptase, CPA3 staining. Expression of Tryptase and CPA3 in 29 matched pre- and post-NACT tumors and corresponding secondary only, negative control taken at a 20x that were used for quantification of tryptase and CPA3 positive cells

Supplementary Material 4: Supplementary Figure 4. Representative immunofluorescence images of Tryptase, CPA3 staining. Expression of Tryptase and CPA3 in 29 matched pre- and post-NACT tumors and corresponding secondary only, negative control taken at a 20x that were used for quantification of tryptase and CPA3 positive cells

Supplementary Material 5: Supplementary Figure 5. Hematologic identified mast cell levels association with progression-free survival. Kaplan-Meier survival curve analysis of post-NACT (A) total, (B) stromal, and (C)intraepithelial mast cell levels association with progression-free survival stratified by upper and lower quartile. HR and associated log-rank p-values were reported. NACT, neoadjuvant chemotherapy; HR, hazard ratio

Supplementary Material 6: Supplementary Figure 6. Hematologic identified mast cell levels association with overall survival. Kaplan-Meier survival curve analysis of post-NACT (A) total, (B) stromal, and (C) intraepithelial mast cell levels association with overall survival stratified by upper and lower quartile. HR and associated log-rank p-values were reported. NACT, neoadjuvant chemotherapy; HR, hazard ratio

Supplementary Material 7: Supplementary Figure 7. Tryptase+/CPA3+ mast cells association with overall survival. Kaplan-Meier survival curve analysis of post-NACT (A) total, (B) stromal, and (C) intraepithelial mast cell levels association with overall survival stratified by upper and lower quartile. HR and associated log-rank p-values were reported. NACT, neoadjuvant chemotherapy; HR, hazard ratio

Supplementary Material 8: Supplementary Figure 8. Tryptase+ mast cells association with overall survival. Kaplan-Meier survival curve analysis of post-NACT (A) total, (B) stromal, and (C) intraepithelial mast cell association with overall survival stratified by median levels. HR and associated log-rank p-values were reported. NACT, neoadjuvant chemotherapy; HR, hazard ratio

Supplementary Material 9: Supplementary Figure 9. Intraepithelial and Stromal Tryptase+ mast cells association with overall survival. Kaplan-Meier survival curve analysis of post-NACT (A) intraepithelial and (B) stromal mast cells association with overall survival stratified by lower and upper quartile levels. HR and associated log-rank p-values were reported. NACT, neoadjuvant chemotherapy; HR, hazard ratio

Supplementary Material 10: Supplementary Figure 10. Tryptase+ mast cells association with progression-free survival. Post-NACT (A) total, (B) intraepithelial, and (C) stromal Tryptase+/CPA3+ levels stratified by progression-free survival 12-month cut-off. Statistical significance determined by Student T-test. NACT, neoadjuvant chemotherapy; ns, non-significant

Supplementary Material 11: Supplementary file 1

Acknowledgements

The authors would like to thank Dr. Richard Freiman and Dr. Kathryn Grive for the gracious allowance of their microscopes to be utilized for this study.

Author contributions

JM and NJ: Conceptualization and Design. JM, JE, DM, CJ, NJ: Data Acquisition, Analysis, and Interpretation. JO and LCH: FFPE tissue acquisition and quality assessment. JM and NJ: Manuscript Writing. PDLC and NJ: Statistical Analysis. NJ: Funding acquisition. All authors reviewed and approved the final manuscript version.

Funding

This study was funded by Swim Across America, Lura Cook Hull Trust, the Kilguss Core of Women and Infants Hospital, Advance CTR, Institutional Development Award Networks for Clinical and Translational Research (IDeA-CTR) from the National Institute of General Medical Sciences (U54GM115677), and the Division of Gynecologic Oncology, Program in Women's Oncology at Women and Infants Hospital.

Data availability

No datasets were generated or analysed during the current study.

Declarations

Ethics statement

This retrospective study using previously collected human biospecimens was reviewed and approved by the Women and Infant Hospital Institutional Review Board (1817644-11). No participants were contacted during the course of the study, and the ethics committee waived the requirement of written informed consent.

Competing interests

The authors declare no competing interests.

Author details

[1]Program in Women's Oncology, Women and Infants Hospital, Providence, RI, USA

[2]Women and Infants Hospital, Department of Obstetrics and Gynecology, Program in Women's Oncology, Warren-Alpert Medical School of Brown University, 200 Chestnut Street, Room 208, Providence, RI 02903, USA
[3]School of Public Health, Brown University, Providence, RI, USA
[4]Department of Pathobiology, Brown University, Providence, RI, USA
[5]Department of Pathology, Women and Infants Hospital, Providence, RI, USA

Received: 24 June 2024 / Accepted: 13 September 2024
Published online: 28 September 2024

References

1. Luvero D, Plotti F, Aloisia A, Montera R, Terranova C et al. Carlo De Cicco Nardone,. Ovarian cancer relapse: From the latest scientific evidence to the best practice. Crit Rev Oncol Hematol. 2019;140:28–38.
2. James NE, Woodman M, DiSilvestro PA, Ribeiro JR. The Perfect Combination: enhancing patient response to PD-1-Based therapies in epithelial ovarian Cancer. Cancers (Basel). 2020;12(8):2150.
3. Zhang L, Conejo-Garcia JR, Katsaros D, Gimotty PA, Massobrio M, Regnani G, et al. Intratumoral T cells, recurrence, and survival in epithelial ovarian cancer. N Engl J Med. 2003;348(3):203–13.
4. Hwang W-T, Adams SF, Tahirovic E, Hagemann IS, Coukos G. Prognostic significance of tumor-infiltrating T cells in ovarian cancer: a meta-analysis. Gynecol Oncol. 2012;124(2):192–8.
5. James NE, Woodman M, De La Cruz P, Eurich K, Ozsoy MA, Schorl C, et al. Adaptive transcriptomic and immune infiltrate responses in the tumor immune microenvironment following neoadjuvant chemotherapy in high grade serous ovarian cancer reveal novel prognostic associations and activation of pro-tumorigenic pathways. Front Immunol. 2022;13:965331.
6. Lichterman JN, Reddy SM. Mast cells: a new frontier for cancer immunotherapy. Cells. 2021;10(6):1270.
7. Oldford SA, Marshall JS. Mast cells as targets for immunotherapy of solid tumors. Mol Immunol. 2015;63(1):113–24.
8. Ebott J, McAdams J, Kim C, Jansen C, Woodman M, De La Cruz P, et al. Enhanced amphiregulin exposure promotes modulation of the high grade serous ovarian cancer tumor immune microenvironment. Front Pharmacol. 2024;15:1375421.
9. Salmon H, Donnadieu E. Within tumors, interactions between T cells and tumor cells are impeded by the extracellular matrix. Oncoimmunology. 2012;1(6):992–4.
10. Wang S-W, Oh CK, Cho SH, Hu G, Martin R, Demissie-Sanders S, et al. Amphiregulin expression in human mast cells and its effect on the primary human lung fibroblasts. J Allergy Clin Immunol. 2005;115(2):287–94.
11. Oliveira SHP, Lukacs NW. Stem cell factor: a hemopoietic cytokine with important targets in asthma. Curr Drug Targets Inflamm Allergy. 2003;2(4):313–8.
12. Gomez G, Ramirez CD, Rivera J, Patel M, Norozian F, Wright HV, et al. TGF-beta 1 inhibits mast cell fc epsilon RI expression. J Immunol. 2005;174(10):5987–93.
13. Rijnierse A, Koster AS, Nijkamp FP, Kraneveld AD. TNF-alpha is crucial for the development of mast cell-dependent colitis in mice. Am J Physiol Gastrointest Liver Physiol. 2006;291(5):G969–76.
14. Meyer N, Hinz N, Schumacher A, Weißenborn C, Fink B, Bauer M et al. Mast cells retard tumor growth in ovarian cancer: insights from a mouse model. Cancers (Basel). 2023;15(17):4278.
15. Chan JK, Magistris A, Loizzi V, Lin F, Rutgers J, Osann K, et al. Mast cell density, angiogenesis, blood clotting, and prognosis in women with advanced ovarian cancer. Gynecol Oncol. 2005;99(1):20–5.
16. Cao K, Zhang G, Zhang X, Yang M, Wang Y, He M, et al. Stromal infiltrating mast cells identify immunoevasive subtype high-grade serous ovarian cancer with poor prognosis and inferior immunotherapeutic response. Oncoimmunology. 2021;10(1):1969075.
17. Liu M, Zhang Y, Xu Q, Liu G, Sun N, Che H, et al. Apigenin inhibits the Histamine-Induced Proliferation of Ovarian Cancer cells by downregulating ERα/ERβ expression. Front Oncol. 2021;11:682917.
18. de Souza DA, Toso VD, Campos MR, de Lara C, Oliver VS, Jamur C. Expression of mast cell proteases correlates with mast cell maturation and angiogenesis during tumor progression. PLoS ONE. 2012;7(7):e40790.
19. Xiao H, He M, Xie G, Liu Y, Zhao Y, Ye X, et al. The release of tryptase from mast cells promote tumor cell metastasis via exosomes. BMC Cancer. 2019;19(1):1015.
20. Akula S, Hellman L, Avilés FX, Wernersson S. Analysis of the mast cell expressed carboxypeptidase A3 and its structural and evolutionary relationship to other vertebrate carboxypeptidases. Dev Comp Immunol. 2022;127:104273.
21. Atiakshin D, Kostin A, Trotsenko I, Samoilova V, Buchwalow I, Tiemann M. Carboxypeptidase A3-A key component of the protease phenotype of mast cells. Cells. 2022;11(3):570.
22. Serafin WE, Dayton ET, Gravallese PM, Austen KF, Stevens RL. Carboxypeptidase A in mouse mast cells. Identification, characterization, and use as a differentiation marker. J Immunol. 1987;139(11):3771–6.
23. Henningsson F, Hergeth S, Cortelius R, Abrink M, Pejler G. A role for serglycin proteoglycan in granular retention and processing of mast cell secretory granule components. FEBS J. 2006;273(21):4901–12.
24. Gurish MF, Ghildyal N, McNeil HP, Austen KF, Gillis S, Stevens RL. Differential expression of secretory granule proteases in mouse mast cells exposed to interleukin 3 and c-kit ligand. J Exp Med. 1992;175(4):1003–12.
25. Atiakshin D, Patsap O, Kostin A, Mikhalyova L, Buchwalow I, Tiemann M. Mast cell tryptase and carboxypeptidase A3 in the formation of ovarian endometrioid cysts. Int J Mol Sci. 2023;24(7):6498.
26. Grujic M, Paivandy A, Gustafson A-M, Thomsen AR, Öhrvik H, Pejler G. The combined action of mast cell chymase, tryptase and carboxypeptidase A3 protects against melanoma colonization of the lung. Oncotarget. 2017;8(15):25066–79.
27. Ribatti D. Mast cells and resistance to immunotherapy in cancer. Arch Immunol Ther Exp (Warsz). 2023;71(1):11.
28. Li J, Peng G, Zhu K, Jie X, Xu Y, Rao X, et al. PD-1 + mast cell enhanced by PD-1 blocking therapy associated with resistance to immunotherapy. Cancer Immunol Immunother. 2023;72(3):633–45.
29. Somasundaram R, Connelly T, Choi R, Choi H, Samarkina A, Li L, et al. Tumor-infiltrating mast cells are associated with resistance to anti-PD-1 therapy. Nat Commun. 2021;12(1):346.
30. Wroblewski M, Bauer R, Cubas Córdova M, Udonta F, Ben-Batalla I, Legler K, et al. Mast cells decrease efficacy of anti-angiogenic therapy by secreting matrix-degrading granzyme B. Nat Commun. 2017;8(1):269.
31. Sznurkowski JJ. To Bev or not to Bev during ovarian cancer maintenance therapy? Cancers (Basel). 2023;15(11):2980.
32. Nakai H, Matsumura N. The roles and limitations of bevacizumab in the treatment of ovarian cancer. Int J Clin Oncol. 2022;27(7):1120–6.
33. Krist LF, Eestermans IL, Steenbergen JJ, Hoefsmit EC, Cuesta MA, Meyer S, Beelen RH. Cellular composition of milky spots in the human greater omentum: an immunochemical and ultrastructural study. Anat Rec. 1995;241(2):163–74.

Publisher's note